OPEN

Citation: Cell Death and Disease (2013) 4, e819; doi:10.1038/cddis.2013.364

www.nature.com/cddis

Opposing effects of high- and low-molecular weight hyaluronan on CXCL12-induced CXCR4 signaling depend on CD44

K Fuchs[1], A Hippe[2], A Schmaus[1], B Homey[2], JP Sleeman[1,3] and V Orian-Rousseau*[,1]

The tumor microenvironment makes a decisive contribution to the development and dissemination of cancer, for example, through extracellular matrix components such as hyaluronan (HA), and through chemokines that regulate tumor cell behavior and angiogenesis. Here we report a molecular link between HA, its receptor CD44 and the chemokine CXCL12 in the regulation of cell motility and angiogenesis. High-molecular-weight HA (hHA) was found to augment CXCL12-induced CXCR4 signaling in both HepG2iso cells and primary human umbilical vein endothelial cells, as evidenced by enhanced ERK phosphorylation and increased cell motility. The augmentation of CXCR4 signaling translated into increased vessel sprouting and angiogenesis in a variety of assays. Small HA oligosaccharides (sHA) efficiently inhibited these effects. Both siRNA-mediated reduction of CD44 expression and antibodies that block the interaction of CD44 with HA provided evidence that CXCL12-induced CXCR4 signaling depends on the binding of hHA to CD44. Consistently, CD44 and CXCR4 were found to physically interact in the presence of CXCL12, an interaction that could be inhibited by sHA. These findings provide novel insights into how microenvironmental components interact with cell surface receptors in multi-component complexes to regulate key aspects of tumor growth and progression.

Cell Death and Disease (2013) **4,** e819; doi:10.1038/cddis.2013.364; published online 3 October 2013
Subject Category: Cancer

The tumor microenvironment plays a major role in cancer development and progression, and interactions between cancer cells and the microenvironment are essential both for the growth of the primary tumor and for the migration of metastatic cells to distant organs and their survival there.[1] This microenvironment comprises stromal cells such as angiogenic vascular cells, infiltrating immune cells and cancer-associated fibroblasts, together with chemokines, growth factors and other factors released by these and other cells and a variety of extracellular cellular matrix (ECM) components.[2]

A major component of the ECM in the tumor microenvironment is hyaluronan (HA), a high MW ($>10^6$ kDa) non-sulfated glycosaminoglycan consisting of repeating subunits of (β,1-4)-D-glucuronic acid-(β,1-3)-N-acetyl-D-glucosamine.[3] Three hyaluronan synthase (HAS) enzymes are involved in the production of HA (HAS1–3), whereas HA degradation is controlled by hyaluronidases (HYALs), six of which have been identified.[4] Overproduction of HA in tumors such as breast, colorectal, prostate, lung, ovarian and gastric cancers correlates in several cases with malignant progression and poor survival,[5–9] as does high expression of HAS and low expression of HYALs.[10] However, overexpression of HYALs can also correlate with malignancy[7,10–14] and accumulation of HA can decrease tumorigenic potential.[15–18] These contradictory observations can be reconciled by the observation that the concurrent expression of synthesizing and degrading enzymes has the strongest impact on tumor growth and metastasis,[15,16,19] suggesting that increased synthesis coupled to turnover of HA is decisive in this context.

Enhanced synthesis and turnover of HA can result in the local accumulation of small HA oligosaccharides (sHA). sHA has stimulatory effects on a number of biological processes that are not observed with high-molecular-weight HA (hHA). For example, angiogenesis, a key component of tumor growth and progression, can be triggered by sHA through the stimulation of endothelial cell (EC) proliferation, motility and tubule formation (reviewed in Toole[10]). Surprisingly, however, administration of sHA to several types of tumor xenografts inhibited rather than stimulated tumor growth.[20,21] These discrepancies might

[1]Karlsruhe Institute of Technology, Institute of Toxicology and Genetics, Karlsruhe, Campus North, Postfach 3640, Karlsruhe, Germany; [2]Department of Dermatology, University Hospital Düsseldorf, Düsseldorf, Germany and [3]Universitätsmedizin Mannheim, University of Heidelberg, Centre for Biomedicine and Medical Technology Mannheim (CBTM), Mannheim, Germany
*Corresponding author: V Orian-Rousseau, Karlsruhe Institute of Technology, Institute of Toxicology and Genetics, Karlsruhe, Campus North, Postfach 3640, 76021 Karlsruhe, Germany. Tel: +49 721 608 26523; Fax: +49 721 608 23354; E-mail: veronique.orian-rousseau@kit.edu
Keywords: CD44; chemokine; angiogenesis; hyaluronan
Abbreviations: BMC, bone marrow cell; EC, endothelial cell; ECM, extracellular matrix; EPC, endothelial progenitor cell; HA, hyaluronan; HAS, hyaluronan synthase; HGF, hepatocyte growth factor; hHA, high-molecular-weight hyaluronan; HSC, hematopoietic stem cell; HUVEC, human umbilical vein endothelial cell; HYAL, hyaluronidase; RTK, receptor tyrosine kinase; sHA, small fragment hyaluronan; TGFα, transforming growth factor α; PTX, pertussis toxin; VEGFR-2, vascular endothelial growth factor 2
Received 11.6.13; accepted 06.8.13; Edited by G Ciliberto

suggest a context-dependent response to HA, influenced by the local environment.

The CD44 family of transmembrane glycoproteins is a major class of cell surface receptors for HA that controls differentiation, proliferation, survival and migration of cells, and thereby has an important role in tumor progression and metastasis.[22] Ample evidence also implicate CD44 in the regulation of angiogenesis. *In vitro*, a CD44 antibody blocked EC proliferation and tube formation.[23] Consistently, vascularization of matrigel implants and tumor and wound angiogenesis were drastically reduced in CD44-knockout mice.[24] Furthermore, the CD44v6 isoform on ECs collaborates with vascular endothelial growth factor 2 (VEGFR-2), a central regulator of angiogenesis, and thereby fosters activation of VEGFR-2. The ectodomain of CD44v6 is required for the activation process, and the cytoplasmic domain controls signaling from VEGFR-2.[25] Accordingly, tumor angiogenesis was blocked by a CD44v6 peptide in this study.

Other components of the tumor microenvironment that induce angiogenesis are the chemokine CXCL12 (SDF-1α) and its receptor CXCR4. CXCL12 stimulates angiogenesis directly by acting on ECs, as they express CXCR4 (reviewed in Salcedo and Oppenheim[26]). CXCL12 is also involved in other aspects of vascular remodeling, for example, by attracting bone marrow-derived CXCR4-positive endothelial progenitor cells (EPCs) to the sites of vessel injury.[27] This latter role for CXCR4 and its ligand in directing the 'homing' of cells to particular organ microenvironments is also important for the migration to and the settlement and retention of hematopoietic stem cells (HSCs) in the bone marrow.[28] Also during metastatic dissemination, CXCR4-expressing metastatic cells home to organs that express CXCL12 (reviewed in Burger and Kipps[29]).

The migration of HSCs to the bone marrow is also dependent on HA/CD44 interactions.[28] HA is highly expressed in sinusoidal endothelium and in the endosteum, a region adjacent to the bone, where primitive HSCs are present. Blocking CD44–HA interaction prevents the settlement of HSCs in these regions. Furthermore, the migration of leukemic stem cells to the bone marrow niche requires both CD44 and CXCR4/CXCL12, as antibodies against either CXCR4 or CD44 can block this migration.[30]

Prompted by the similarities between the effects of CXCR4/CXCL12 signaling and HA/CD44 interactions in a variety of settings, in this study we discovered a regulatory interplay between CD44, HA, CXCR4 and CXCL12 operating in both tumor cells and ECs. We show that the activation of CXCR4 by CXCL12 is increased upon preincubation of cells with hHA. In stark contrast, sHA fragments block CXCL12 signaling. The effects of HA on CXCR4 signaling are dependent on CD44. A complex formed between CXCR4 and CD44 in the presence of CXCL12 was abrogated by preincubation with sHA. Vessel sprouting and aortic ring assays *in vitro*, as well as matrigel plug assays *in vivo* demonstrate a dependence of CXCL12/CXCR4 signaling on HA and CD44 in angiogenesis. Together these data reveal a novel mechanism through which HA in the microenvironment can influence tumor cell behavior and regulate angiogenesis.

Results

Opposing effects of hHA and sHA on CXCR4-induced signaling and cell motility. Possible effects of HA on CXCL12-induced signaling were examined using the CXCR4-positive hepatoma cell line HepG2iso[31] and primary human ECs (HUVECs). Both cell types express CXCR4 (Figure 1a) and the major HA receptor CD44. Hermes 3, an antibody that recognizes all CD44 isoforms, detected several bands in HepG2iso cells and HUVECs. The major band corresponds to CD44s, the smallest ubiquitously expressed CD44 isoform (reviewed in Orian-Rousseau[32]). The upper bands correspond to other CD44 isoforms expressed at lower levels. HepG2 cells that do not express any CD44 isoform served as a negative control (Figure 1a and Olaku *et al*.[33]).

hHA and sHA have been reported to exert differing effects on tumor growth, angiogenesis and inflammation. We therefore examined the effect of hHA and sHA of 6–10 disaccharides in length on CXCL12-induced signaling using phosphorylation of Erk as a read-out (Figure 1b). HepG2iso cells were induced with CXCL12 alone or incubated with increasing amounts of hHA before induction with CXCL12. CXCL12 alone induced Erk phosphorylation. In comparison, hHA treatments at concentrations ranging from 50 to 400 μg/ml further augmented CXCL12-induced Erk phosphorylation. The effect of hHA was best seen at 400 μg/ml, a concentration used for further experiments. In HUVECs, CXCL12 also induced Erk phosphorylation, a response that was further enhanced by preincubation with 400 μg/ml hHA. In stark contrast, sHA decreased CXCL12-induced Erk phosphorylation in both HepG2iso cells and HUVECs, with pronounced inhibition at 1 μg/ml (Figure 1b). Note that given the difference in molecular weight between hHA and sHA, a concentration of 1 μg/ml sHA equates approximately to 400 μg/ml hHA at the molar level.

To investigate whether the effects observed with hHA were due to an activation of the $G_{\alpha i}$ subunit, a G protein involved in CXCR4 signaling (reviewed in Teicher and Fricker[34]), we repeated the previous experiment in the presence or the absence of pertussis toxin (PTX), a specific inhibitor of this subunit.[35] The effects of hHA on CXCL12-induced Erk phosphorylation were completely abrogated by this drug (Figure 1c), indicating that the action of hHA is mediated through the $G_{\alpha i}$-induced Erk pathway.

The effects of hHA and sHA on CXCR4 signaling were further examined using *in vitro* monolayer wound closure assays. A wound of defined size was generated in confluent monolayers of HepG2iso cells. Migration of cells to fill the wound upon induction with CXCL12 alone strongly and significantly increased wound closure after 24 h (Figure 1d). This effect was potently augmented by preincubation with hHA in a statistically significant manner. Preincubation with hHA or sHA alone had no effect on wound closure compared with non-treated control cells. Consistent with the inhibitory effect of sHA on CXCL12-induced Erk phosphorylation, preincubation with sHA completely inhibited the augmented wound closure in response to CXCL12 (Figure 1d).

Similar experiments were performed with HUVECs. Spontaneous wound closure was faster than that observed with HepG2iso cells. Nevertheless, a statistically significant increased wound closure in the presence of CXCL12 was

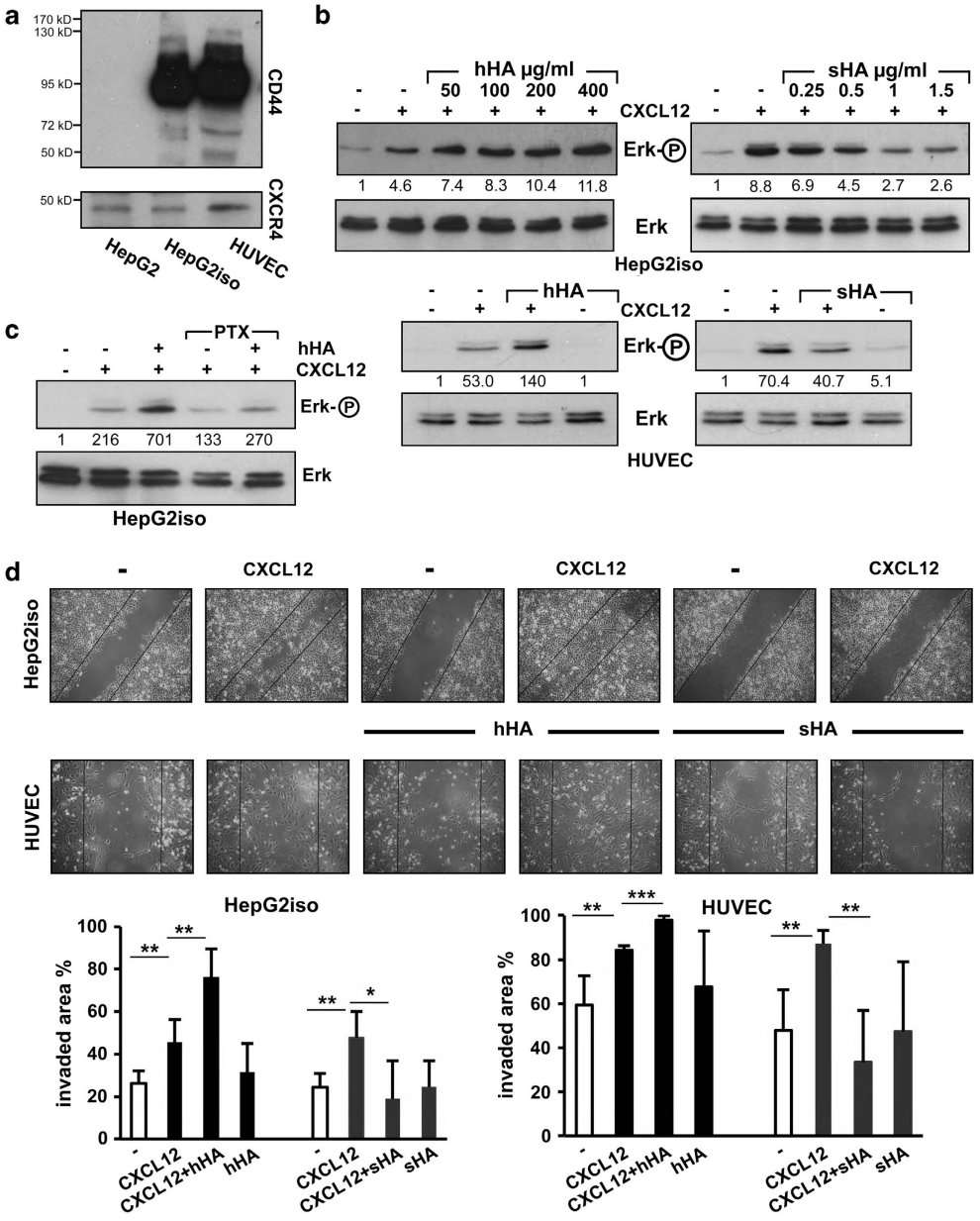

Figure 1 HA modulates CXCL12 signaling and migration. (**a**) Expression of CD44 and CXCR4 in HepG2, HepG2iso cells and HUVECs was evaluated by western blot analysis using a panCD44-specific antibody (Hermes 3) and a CXCR4-specific antibody (ab2074). The apparent molecular weights are indicated. (**b**) CXCL12-induced Erk phosphorylation was evaluated using a phospho-Erk-specific antibody to probe western blots of lysates from HepG2iso cells and HUVECs treated with the indicated compounds. Erk staining was used as loading control. Where indicated, the cells were preincubated with increasing concentrations of high-molecular-weight HA (hHA) or small HA oligosaccharides of 6–10 disaccharides in length (sHA). A similar experiment was performed with HUVECs using 400 μg/ml hHA and 1 μg/ml sHA. These concentrations were used in all subsequent experiments. The numbers between the Erk and phospho-Erk panels indicate fold induction. (**c**) CXCL12-induced phosphorylation of Erk in HepG2iso cells in the absence or presence of hHA and PTX as indicated. The toxin was applied to the cells at 500 ng/ml, 10 min before induction with CXCL12. (**d**) Monolayer wound assays performed with HepG2iso cells and HUVECs in the presence or absence of CXCL12, hHA and sHA as indicated. The upper panel shows representative images of wound closure after 24 h under the indicated conditions using a Canon Power Shot S620 digital camera connected to an Axiovert 40c Zeiss microscope ($\times$ 10 objective). The black lines indicate the wound border immediately after monolayer wounding. The lower panels show quantification of the wound closure using the computer program ImageJ (NIH). Experimental data are reported as mean $\pm$ S.D. of five independent experiments (*$P<0.05$; **$P<0.01$; ***$P<0.005$; Student's *t*-test)

observed after 24 h, which was further and significantly augmented by preincubation with hHA. In addition, sHA inhibited CXCL12-induced migration (Figure 1d). Proliferation assays revealed that CXCL12 did not induce proliferation of either HepG2iso cells or HUVECs to any significant extent during the time period of the wound closure assay (data not shown), ruling out that CXCL12 and hHA might induce monolayer wound closure by promoting cell proliferation.

Opposing effects of hHA and sHA on CXCR4 activity in angiogenesis assays *in vitro*. CXCR4/CXCL12 mediates angiogenesis, vascular remodeling and regeneration by

inducing the recruitment of EPCs to existing vessels or by acting directly on ECs (reviewed in Ho *et al*.[36]). In order to examine the contribution of HA in CXCL12-dependent angiogenesis *in vitro*, we performed a fibrin bead sprouting assay using HUVECs (Figure 2a). The length of vessel-like structures built by ECs attached to the beads was significantly enhanced by treatment with CXCL12, and was further increased in a statistically significant manner by treatment with CXCL12 and hHA together (Figure 2a). In contrast, sHA totally blocked the enhanced sprouting induced by CXCL12, whereas hHA and sHA had no effect on sprouting in the absence of CXCL12 (Figure 2a).

The effect of sHA on CXCL12-induced sprouting was further analyzed using aortic ring assays (Figure 2b). Sprouting from aortic rings requires proliferation, migration of ECs, tube formation, branching and pericyte recruitment, and therefore provides a relevant measure of angiogenesis *ex vivo*. Aorta from C57BL/6 mice were isolated, cut into pieces and embedded in collagen gels. CXCL12 significantly enhanced the outgrowth of blood vessels from aortic rings after 9 days of culture, an effect that was completely inhibited by concomitant treatment with sHA (Figure 2b). Note that the high viscosity of hHA and collagen admixes did not allow aortic ring assays to be performed in the presence of hHA.

CD44 mediates the effect of HA on CXCL12-induced signaling. CD44, the principal HA receptor,[37] can bind to sHA fragments with a minimum size of six HA residues corresponding to three disaccharide subunits.[38] To investigate whether CD44 mediates the effects of HA on the CXCL12-CXCR4 pathway, we repressed expression of all CD44 isoforms in HepG2iso cells using siRNA, then measured the induction of Erk phosphorylation upon CXCL12 treatment either alone or together with hHA (Figure 3a). In control siRNA-transfected cells, Erk phosphorylation was induced upon CXCL12 treatment, a response that was further increased upon preincubation with hHA before CXCL12 treatment, as expected from the data in Figure 1. Repression of CD44 expression dramatically decreased the effect of hHA on CXCL12-induced Erk phosphorylation, suggesting that CD44 mediates the ability of hHA to augment CXCR4 signaling. Repression of CD44

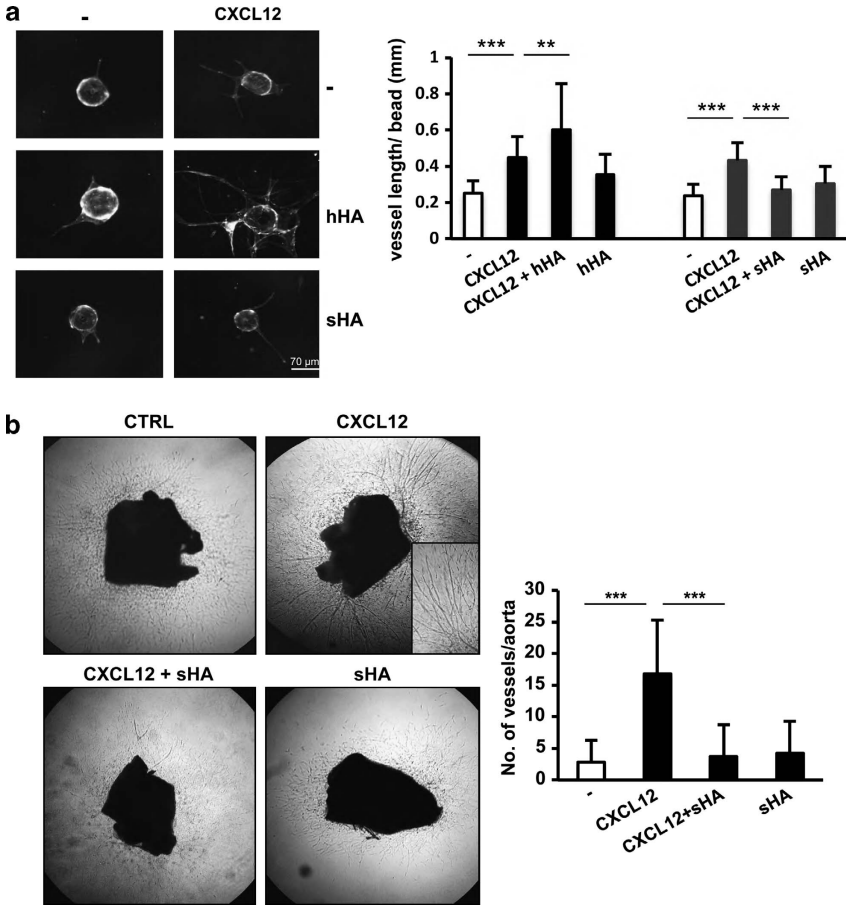

Figure 2 HA modulates CXCL12-induced angiogenesis. (**a**) Sprouting of HUVECs seeded on beads and embedded in fibrinogen in the presence of CXCL12, hHA and sHA as indicated. Left panel: representative pictures were taken with an Olympus IX81 confocal microscope (× 2 objective) after 10 days of culture. Right panel: quantification of sprouting from eight independent experiments (mean ± S.D.) assessed by evaluating the total vessel length per bead using the computer program ImageJ. (**b**) Vessel outgrowth from mouse-derived aorta-pieces treated with CXCL12 and sHA as indicated. Pictures were taken on day 10 using a Canon Power Shot S620 digital camera connected to an Axiovert 40c Zeiss microscope (× 5 objective). Quantification was carried out by counting the number of vessels that grew out. Data were analyzed using ImageJ. Experimental data are reported as mean ± S.D. of five independent experiments. Each data point represent the outgrowth from 15 aorta pieces taken from five mice (**$P<0.01$; ***$P<0.005$; Student's *t*-test)

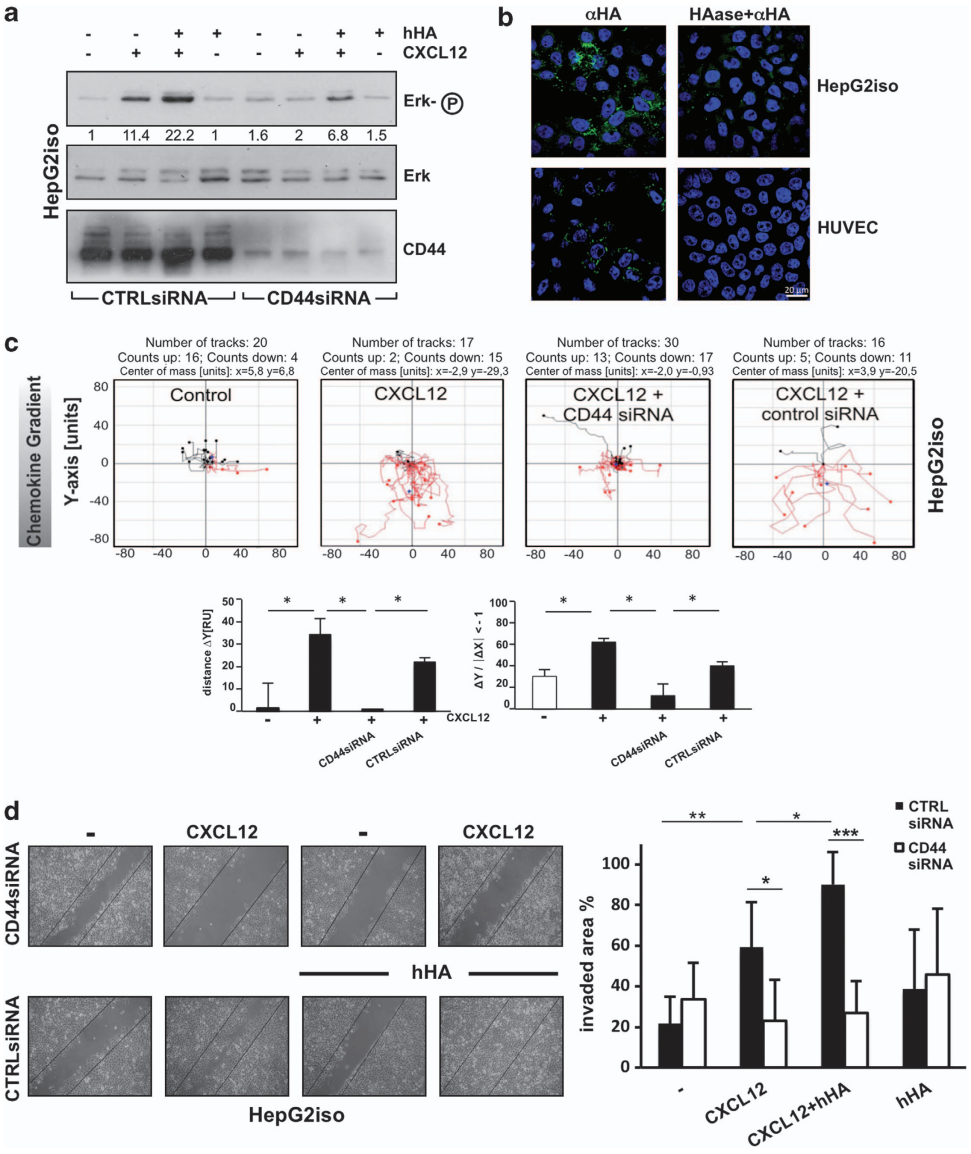

Figure 3 CD44 is required for hHA-modulated CXCL12 signaling and directional migration. (**a**) HepG2iso cells were transiently transfected with panCD44 siRNA (CD44 siRNA) or control siRNA (ctrl siRNA) as indicated. Erk phosphorylation upon treatment of the cells with CXCL12 and/or hHA as indicated as well as total Erk levels were determined using western blot analysis. (**b**) HA staining (green fluorescence) of serum-starved HepG2iso cells and HUVECs was performed using a biotinylated HA-binding protein (αHA). Nuclei were counterstained with DAPI (blue fluorescence). Images were taken with a SpE confocal microscope (Leica, × 63 magnification). As a control, cells were pretreated with hyaluronidase (HAase) before staining (right panel). (**c**) Upper panel: representative trajectories of HepG2iso cells cultured inside an IBIDI μ chemotaxis chamber containing CXCL12 (200 ng/ml) or PBS as a control. Cell were transfected either with 5 nM CD44-specific siRNA (CD44 siRNA) or control siRNA (ctrl siRNA) as indicated. Lower panel: statistical analysis of the HepG2iso cell trajectories in three independent experiments (mean ± S.D.): average ΔY, mean net distance (RU) traveled along the chemokine gradient (*y* axis). $\Delta Y/|\Delta X| < -1$, percentages of HepG2iso cells traveling a longer distance in the direction of chemokine gradients (*y* axis) than in the direction orthogonal to the gradients (*x* axis) (*$P \leq 0.05$; Student's *t*-test). Migration of the cells is observed for 60 h with a Zeiss Cell Observer. Data were analyzed using ImageJ. (**d**) Representative example of monolayer wound assays performed with HepG2iso cells transiently transfected with panCD44 siRNA (CD44 siRNA) or control siRNA (ctrl siRNA). The cells were treated with CXCL12 and hHA as indicated. Left panel: representative pictures taken 24 h after monolayer wounding using a Canon Power Shot S620 digital camera connected to an Axiovert 40c Zeiss microscope (× 5 objective). The black lines indicate the wound border immediately after monolayer wounding. Quantification of wound closure from six independent experiments using the computer program ImageJ is shown in the right panel. The error bars represent the mean ± S.D. (*$P < 0.05$; **$P < 0.01$; ***$P < 0.005$; Student's *t*-test)

expression also attenuated the ability of CXCL12 to induce Erk phosphorylation in the absence of exogenously added hHA (Figure 3a). As HepG2iso cells clearly synthesize HA (Figure 3b), this suggests that CXCL12-induced CXCR4 signaling is also regulated by CD44 through the action of endogenously produced HA.

To further demonstrate an involvement of CD44 in the HA-mediated regulation of CXCR4 signaling, we performed a chemotaxis assay using ibidi chambers to assess directed migration of HepG2iso cells toward a CXCL12 gradient (Figure 3c). In the absence of CXCL12, the motility of the cells was very low. CXCL12 acted as a chemoattractant for

the HepG2iso cells, but this effect was abrogated by siRNA-mediated downregulation of CD44 expression (Figure 3c). Monolayer wound assays were also performed with HepG2iso cells (Figure 3d). As expected from Figure 1, CXCL12 significantly increased wound closure in control siRNA-transfected cells, an effect that was further significantly augmented by concomitant incubation with hHA. However, in HepG2iso cells depleted for CD44, neither CXCL12 alone nor in combination with HA induced migration of cells and wound closure over and above that observed in non-treated cells (Figure 3d).

To further substantiate the notion that binding of hHA to CD44 is required for CXCL12-induced CXCR4 signaling, we used the BU52 antibody that blocks the binding of HA to CD44. In the presence of BU52, CXCL12-induced Erk phosphorylation in HepG2iso cells was drastically reduced (Figure 4a). No inhibition was observed in the presence of an IgG control. This effect is specific to CXCL12-induced signaling, as transforming growth factor α (TGFα)-induced Erk activation was not affected by the BU52 antibody. The migration of HepG2iso cells and HUVECs was also measured in the presence or absence of the BU52 antibody using monolayer wound closure assays. For both cell types, BU52 completely abrogated migration in response to CXCL12 or CXCL12 and hHA, whereas an IgG control antibody had no effect (Figures 4b and c). Thus, the binding of CD44 to HA is necessary for CXCL12-induced CXCR4 signaling. The migration observed in the presence of CXCL12 alone might be due to the endogenous HA production by HUVECs (Figure 3b).

The role of CD44 in CXCL12-induced angiogenesis was examined in aortic ring assays. The anti-murine CD44 antibody KM81 that inhibits the binding of HA to CD44[39] completely abrogated the ability of CXCL12 to induce vessel sprouting in a statistically significant manner (Figure 5a).

These data indicate that the effects of HA on CXCL12-induced CXCR4 signaling are mediated by CD44. We therefore tested whether CXCR4 and CD44 can physically associate. Indeed, CD44 was detected in lysates of HepG2iso cells and HUVECs immunoprecipitated with an anti-CXCR4 antibody (Figure 5b). In similar experiments, CXCR4 was detected in immunoprecipitates of CD44. The association between CXCR4 and CD44 was dependent on the presence of CXCL12 (Figure 5b). Importantly, formation of the

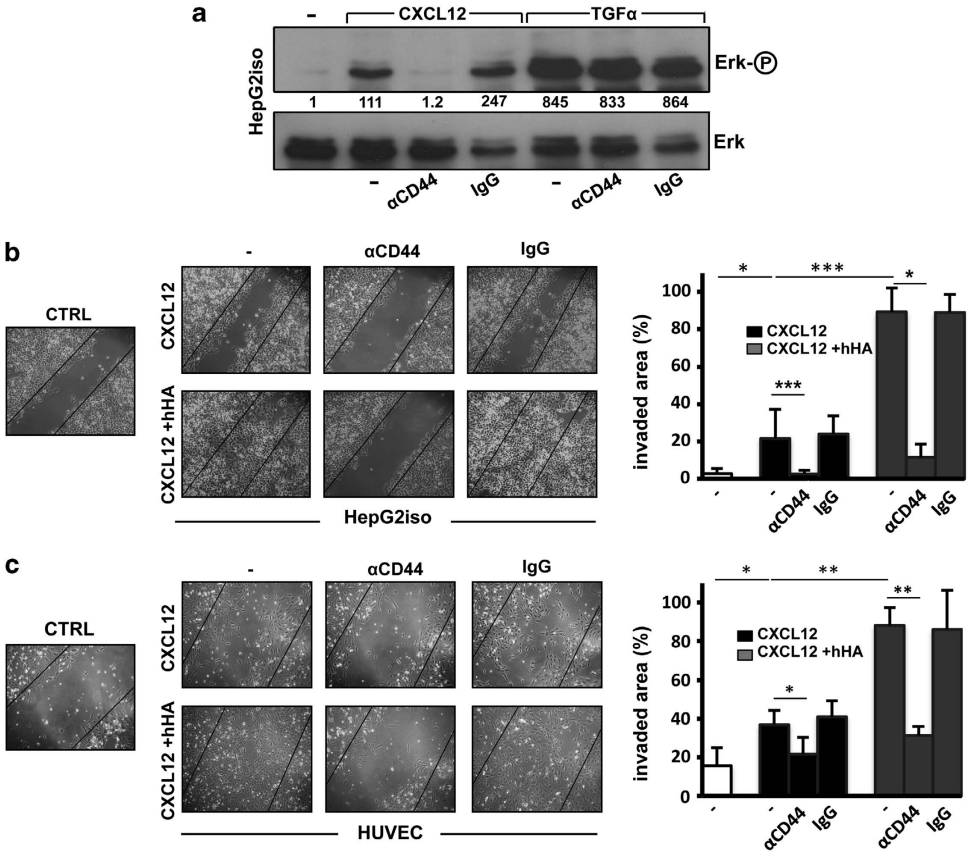

Figure 4 Binding of HA to CD44 is required for CXCL12 signaling. (**a**) Erk phosphorylation induced by CXCL12 or TGFα in HepG2iso cells in the presence or absence of the BU52 antibody (αCD44) that blocks HA binding by CD44 was evaluated using western blot analysis. IgG served as a negative control. Total Erk levels served as a loading control. The numbers between the Erk and phospho-Erk panels indicate fold induction of Erk phosphorylation. (**b** and **c**) Monolayer wound assays using confluent monolayers of HepG2iso cells (**b**) and HUVECs (**c**) in the presence of CXCL12, hHA, the BU52 antibody (αCD44) or an IgG control as indicated. The left panels show representative pictures taken 24 h after monolayer wounding using a Canon Power Shot S620 digital camera connected to an Axiovert 40c Zeiss microscope ($\times$ 10 objective). The black lines indicate the wound border immediately after monolayer wounding. Experimental data are reported as mean $\pm$ S.D. of three independent experiments shown in the right panels (*$P<0.05$; **$P<0.01$; ***$P<0.005$; Student's *t*-test)

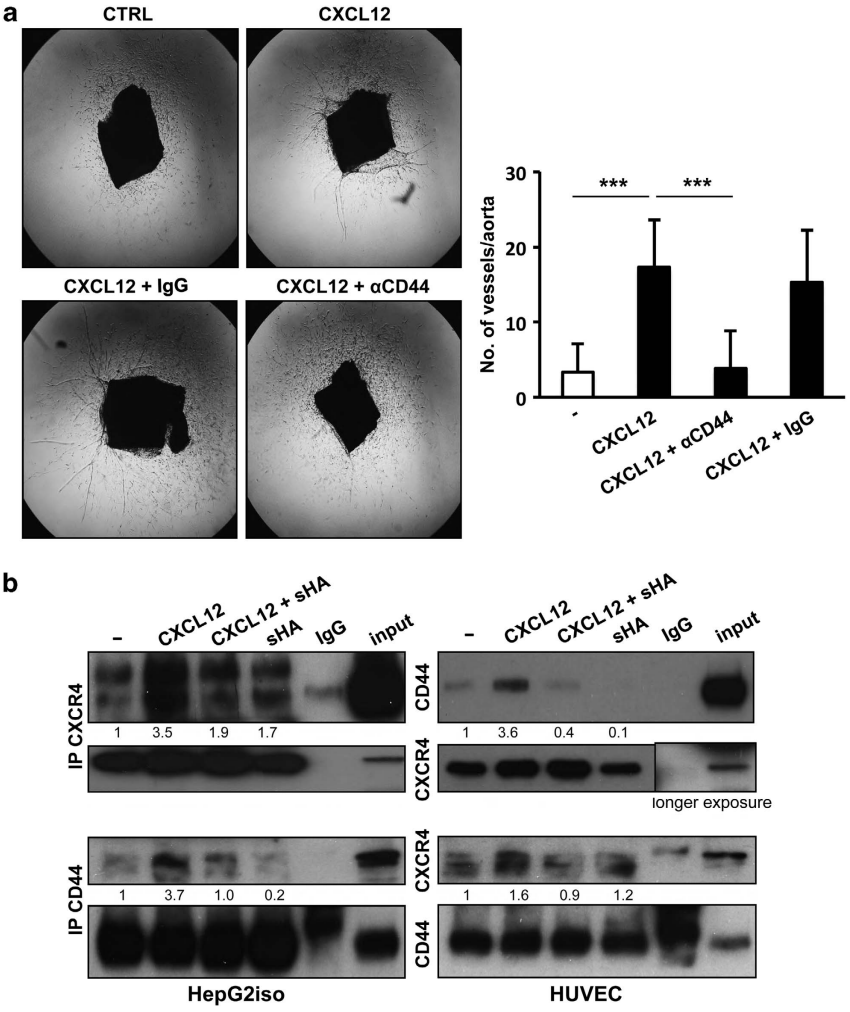

Figure 5 Binding of HA to CD44 is required for CXCL12-induced vessel formation. (**a**) Mouse-derived aorta pieces embedded in collagen were treated with CXCL12 and KM81 CD44 antibodies that block HA binding to CD44 (αCD44) or with IgG as indicated. The left panel shows representative pictures of vessel outgrowth taken after 10 days using a Canon Power Shot S620 digital camera connected to an Axiovert 40c Zeiss microscope and evaluated using ImageJ. The right panel shows quantification of vessel outgrowth. Experimental data are reported as mean ± S.D. of four independent experiments. Each data point represents 11 aorta pieces from four independent mice. (***$P<0.005$; Student's *t*-test). (**b**) Coimmunoprecipitation of CD44 and CXCR4 using lysates from HepG2iso cells (left panels) and HUVECs (right panels) that had been treated with CXCL12 and sHA as indicated. In each case, the samples in the two upper panels were immunoprecipitated with CXCR4 antibodies (IP CXCR4), and the samples in the two lower panels were immunoprecipitated with CD44 antibodies (IP CD44). The western blots were probed with either CD44 or CXCR4 antibodies as indicated between the left and right panels. Negative control immunoprecipitations were performed using IgG. The lanes labeled 'Input' contain a sample of the lysate that was used for the immunoprecipitations. Where indicated, western blots were exposed for longer times to reveal weak signals

CXCR4–CD44 complex was inhibited by preincubation with sHA. These results suggest that sHA exerts its inhibitory effects by preventing the formation of a complex between CD44 and CXCR4 in the presence of CXCL12. Conversely, these data also suggest that hHA fosters complex formation between CXCL12, CD44 and CXCR4, and that this complex is required for downstream signaling to Erk.

Activation of CXCL12-dependent signaling by hHA drives angiogenesis *in vivo*. The role of HA and CD44 in CXCL12-induced angiogenesis *in vivo* was examined using a mouse angiogenesis assay in which the ingrowth of vessels into a subcutaneous matrigel plug is evaluated. CXCL12 either alone or in combination with sHA or hHA was mixed with matrigel and then injected into the flanks of C57/BL6 mice (Figure 6a). Each animal was injected with a control matrigel plug on one flank and a plug containing CXCL12 alone or in combination with hHA or sHA on the other side. Vascularization of the matrigel plugs after 3 weeks in the mice was evaluated by quantifying blood vessels in sections of the plugs using CD31 immunostaining (Figure 6a). As expected, CXCL12 was able to significantly enhance vascularization of the matrigel plugs, an effect that was further significantly augmented in matrigel plugs containing a mixture of hHA and CXCL12. In contrast, only few blood vessels were detected in the presence of sHA, comparable to the number observed in the absence of growth factor addition. The same experiment was performed in the presence of the KM81 antibody that prevents the binding of HA to CD44 (Figure 6b). This antibody dramatically and

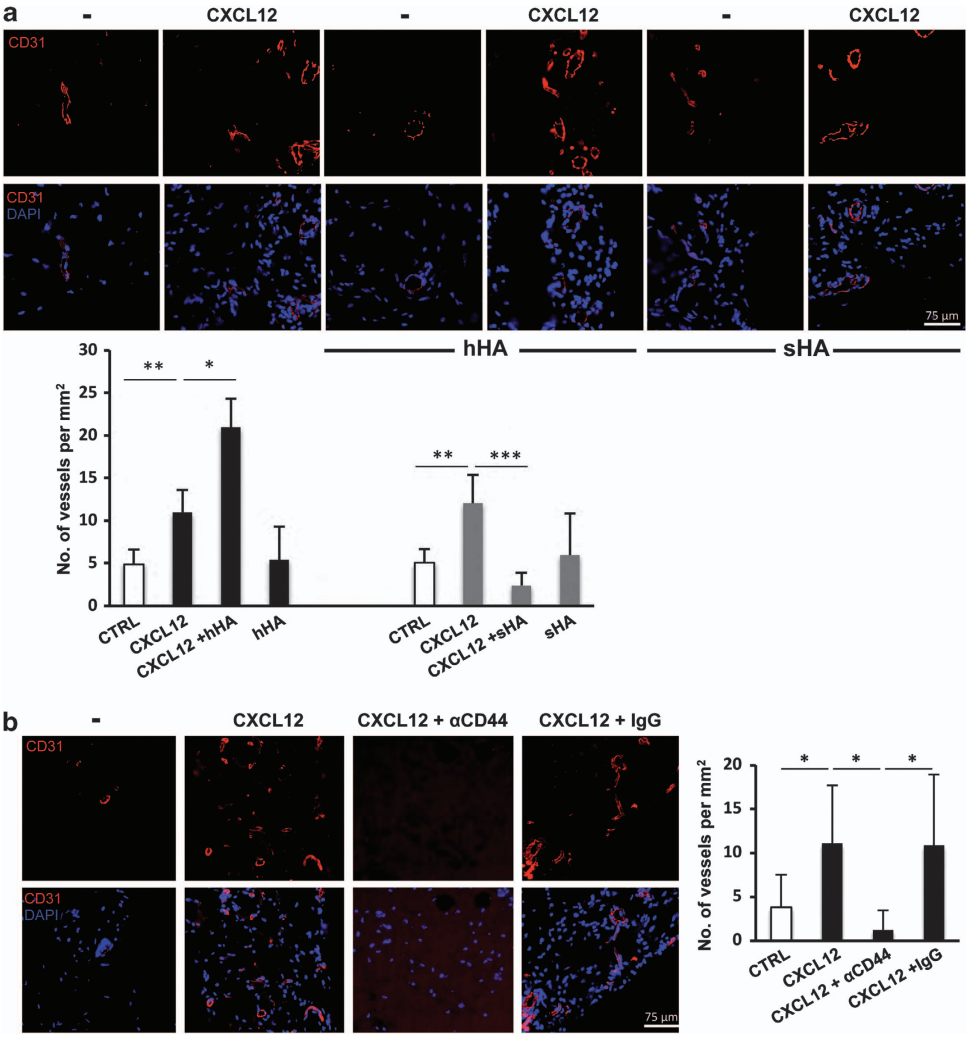

Figure 6 Formation of blood vessels *in vivo* is induced by CXCL12 and can be modulated by HA. (**a**) CXCL12, hHA and sHA as indicated were mixed with matrigel and injected subcutaneously into mice. Vascularization of the plugs after 21 days in the mice was evaluated by sectioning the plugs and staining them with anti-CD31 antibodies (red fluorescence). The sections were also counterstained with DAPI (blue fluorescence) to label cell nuclei. The upper panels show representative pictures of the stained plug sections. Images were taken using a Leica DM5500 microscope ($\times$ 20 objective). The number of CD31-positive vessels in the plugs per mm^2 was then evaluated. The scale bar represents 75 μm. The lower panel shows quantification of the data, with each data point representing the mean number of vessels per mm^2 from five independent plugs. (**b**) Matrigel plug assays identical to those in **a** were performed, except that the matrigel was mixed with CXCL12, the CD44 antibody KM81 or an IgG control as indicated. Representative pictures of stained plug sections (left panel) and vessel quantification (right panel) as described for **a** are shown. Experimental data are reported as mean ± S.D. of five independent plugs. (*$P<0.05$; **$P<0.01$; ***$P<0.005$; Student's *t*-test)

significantly blocked the formation of blood vessels in the matrigel plugs as compared with an IgG control. These *in vivo* data validate the role of HA and CD44 in regulating CXCL12-dependent angiogenesis.

Discussion

In this paper, we show that hHA promotes CXCL12-induced CXCR4 activation, whereas sHA fragments of 6–10 disaccharides in length inhibit CXCR4-induced Erk phosphorylation. These opposing effects were also observed in the CXCL12-induced angiogenesis in both *ex vivo* and *in vivo* assays. hHA fosters CXCR4 signaling through CD44, because both knockdown of CD44 and the blocking of HA binding to CD44 inhibited augmentation of CXCL12-induced signaling and migration in response to hHA. The inhibition of complex formation between CD44 and CXCR4 by sHA suggests that the inhibitory effects of sHA are also mediated through CD44.

Our findings have significance for a broad range of physiological and pathological processes involving CXCR4 signaling. In the context of cancer, hHA-augmented CXCR4 signaling could promote tumor cell dissemination by enhancing the motility of CXCR4-positive tumor cells. Furthermore, through promoting angiogenesis, hHA-augmented CXCR4 signaling might foster the growth of tumors and their metastatic spread. The collaboration between CD44, HA, CXCL12 and CXCR4 might also be important for the establishment of a niche for metastatic cells in distant organs. In line with this notion, an HA matrix produced by

CD44v6-positive metastatic tumor cells supports their migration and enhances their resistance to apoptosis.[40] In addition, the survival of metastatic cells in distant organs is inhibited by blocking CD44v6, as a CD44v6 peptide that inhibits the coreceptor function of CD44v6 for the receptor tyrosine kinase (RTK) Met eliminates established metastases in the lungs (our own unpublished data). The survival of metastatic cells in the lungs might rely both on the CD44v6-dependent Met signaling as well as on CXCR4 signaling augmented by CD44 and hHA.

Enhanced angiogenesis through augmented CXCR4 signaling mediated by CD44 and hHA is not only relevant in the tumor context but also in other situations in which CXCR4 promotes vessel growth and repair. CXCL12 can act directly on EC to induce angiogenesis (reviewed in Salcedo and Oppenheim[26]). Although the CXCL12-CXCR4 effect on tumor angiogenesis has been reported to be independent on VEGF,[41] other studies suggest that CXCR4 signaling leads to increased release of VEGF from ECs. In turn, VEGF fosters both CXCR4 and CXCL12 expression in ECs, leading to amplified angiogenic signaling (reviewed in Salcedo and Oppenheim[26]). CXCL12-induced CXCR4 signaling is also involved in the recruitment of EPCs to sites of arterial injury, where they participate in regenerative re-endothelialization,[42] a step where CD44 and hHA may be relevant.

Our data also cast light on how CXCR4 regulates homing of cells to particular sites. In particular, the data presented here give a mechanistic insight into how CD44 and HA contribute to the settlement of HSCs and leukemic stem cells in the bone marrow niche, as in both cases blocking of CD44 impaired the CXCL12-induced homing of cells to their niche.[28,30] Similarly, migration of bone marrow cells (BMCs) to sites of myocardial infarction can be induced by incorporation of CXCL12 into HA hydrogels implanted into the infarction sites.[43] Consistent with our observations, this study found that the sustained release of CXCL12 together with HA drastically increased the number of BMCs at the infarction site as compared with the use of CXCL12 alone, leading to increased formation of new blood vessels and improved repair of the damaged organs.

Our data clearly show that CXCR4 and CD44 form a physical complex in a CXCL12-dependent manner. In this complex, hHA could conceivably act in a number of ways to promote CXCR4 signaling. For example, it could induce or stabilize the complex between CXCR4 and CD44, perhaps by inducing clustering of CD44 that might structure the complex. Indeed, FRET analysis has shown that hHA can induce CD44 clustering at the cell surface, an event that is strongly attenuated by addition of sHA.[44] Our observation that sHA interferes with CXCR4 signaling would be consistent with the notion that hHA serves to cluster CD44, thereby fostering complex formation between CD44, CXCR4 and CXCL12. Alternatively or in addition, direct binding of CXCL12 to hHA might explain the influence of HA on CXCR4 signaling, for example, by concentrating CXCL12 in the vicinity of CXCR4. The binding of chemokines to glycosaminoglycans occurs through negative charges present on glycosaminoglycans such as HA that can interact with the positively charged chemokines.[45] Consistent with this notion, the direct binding of HA macromers to CXCL12 has recently been demonstrated.[43] In this scenario, CD44 would promote CXCL12-induced CXCR4 signaling by tethering hHA complexed with CXCL12 in the close vicinity of CXCR4, thereby fostering the interaction between CXCR4 and its ligand. In contrast, sHA would saturate CD44–HA-binding sites non-productively, as its short length would permit binding to CD44 but not concomitant binding to CXCL12.

An anti-angiogenic action for hHA and a pro-angiogenic effect for sHA have been reported.[46] On the other hand, our data suggest that hHA should promote angiogenesis and tumor growth, whereas sHA would have an inhibitory effect. Injection of sHA oligomers into tumor-bearing animals inhibits tumor growth,[21] and at least one of the several HYAL genes that contributes to sHA production corresponds to a previously mapped tumor suppressor gene,[47] possibly consistent with our findings. Moreover, the effects of HA and sHA are likely to be context dependent, particularly with regard to the spectrum of growth factors and chemokines found in a particular microenvironment. Indeed, we have observed opposite effects to the ones described here for hHA and sHA in the case of the RTK Met. In this case, hHA inhibits Met activation, whereas sHA promotes it (our own unpublished results). Differences in the mode of activation of RTKs compared with G-Protein-coupled receptors such as CXCR4 might therefore also contribute to differences in the biological activity of hHA and sHA.

In summary, our data uncover a novel regulatory network through which HA of different sizes has contrasting effects on CXCL12-induced CXCR4 signaling in a CD44-dependent manner. This network provides a framework that allows context-dependent regulation of cell motility and angiogenesis.

Materials and Methods

Cells. Human umbilical vein ECs (HUVECs; Provitro GmbH, Berlin, Germany) were grown in Endothelial Cell Growth medium supplemented with EGM-2 SingleQuot Kit Supplements and Growth Factors (Lonza GmbH, Basel, Switzerland). ECs were used at less than 10 passages. The human liver carcinoma cell lines HepG2 (ATCC) and HepG2iso[31] were grown in DMEM (Invitrogen, Darmstadt, Germany) supplemented with 10% FCS (PAA Laboratories, Coelbe, Germany).

Reagents. The antibodies used in this study were directed against human CD44 (Hermes 3, gift from S Jalkannen, Turku, Finland) and BU52 (Pierce, Rockford, IL, USA)), mouse CD44 (KM81 from ATCC), human CXCR4 (ab2074 from Abcam, Cambridge, UK), Erk (K-23 from Santa Cruz Biotechnology, Dallas, TX, USA) and Erk phospho-p44/42 (Cell Signaling Technology, Boston, MA, USA). The horseradish peroxidase-coupled secondary antibodies were from Dako (Hamburg, Germany), the murine and human CXCL12 and the human TGFα from R&D Systems (Wiesbaden, Germany). Hepatocyte growth factor was a generous gift of George Vande Woude (Van Andel Institute). Healon was from Abbott Medical Optics (Santa Ana, CA, USA). Small HA oligosaccharides (6–10 disaccharides) were prepared as previously described.[48]

siRNA oligonucleotides and transfection. Aliquots of cells (1×10^5) were seeded in 12-well plates and transfected with 5 nM CD44 pan siRNA (SI00012775; SI03037419; SI03062661; Qiagen, Hilden, Germany) or control siRNA (5′-UAAUGUAUUGGAACGCAUAUU-3′; 5′-AGGUAGUGUAAUCGCCUUGUU-3′ and 5′-UGCGCUAGGCCUCGGUUGCUU-3′; Eurofins MWG GmbH, Ebersberg, Germany) using Lipofectamine 2000 (Invitrogen), according to the manufacturer's protocol.

Activation of Erk. Cells were serum-starved for 24 h, then induced with the indicated growth factors (20 ng/ml) for 10 min at 37 °C. Where indicated, the cells were treated with BU52 (3 μg/ml), hHA (400 μg/ml) or sHA (6–10 disaccharides, 1 μg/ml) at 37 °C for 30 min before induction, unless otherwise stated. Activated

Erk was determined and quantified using western blot analysis as previously described.[25]

HA detection. Cells were seeded in 12-well plates on cover slips (2.5×10^5 cells per well) and starved for 24 h. Paraffin sections were stained overnight with biotinylated HA-binding protein (HABP (Merck, Darmstadt, Germany), 2.5 μg/ml). After incubation with Streptavidin/HRP (Invitrogen) for 45 min, nuclei were stained with DAPI (Dako). For controls, cells were incubated with 50 U/ml hyaluronidase (Bovine Testis Hyaluronidase, Sigma, Munich, Germany) before fixation.

Coimmunoprecipitation. HUVECs or HepG2iso cells (1.5×10^6 in 10-cm plates) were stimulated with the indicated ligands. For immunoprecipitation (IP) of CD44, cells were lysed in 50 mM Tris-HCl (pH 7.4), 150 mM NaCl, 1 mM EDTA, 1% Triton-X-100, 0.1% SDS, 1% sodium deoxycholate, 1 mM sodium orthovanadate, 1 mM aprotinin and 1 mM leupeptin. The lysis buffer for the CXCR4 IP was: 0.1% Brij 58, 150 mM NaCl, 20 mM Tris-HCl (pH 8.2), 2 mM EDTA, 1 mM sodium orthovanadate, 1 mM aprotinin and 1 mM leupeptin. Cells were lysed for 30 min on ice, then centrifuged for 20 min at 12 000 *g*. The cleared lysates were incubated with antibody-coated protein A/G agarose beads (Merck). The beads were washed in lysis buffer, then subjected to western blot analysis.

Monolayer wounding assay. Cells were seeded in 12-well plates (2.5×10^5 cells per well). A scratch (monolayer wound) was made in the confluent cell layer 24 h later with a sterile pipette tip. Fresh medium containing 400 μg/ml Healon, 1 μg/ml sHA or 3 μg/ml BU52 was added as indicated. After 10 min at 37 °C, induction with CXCL12 (20 ng/ml) was performed where indicated.

Chemotactic cell migration. Chemotactic cell migration assays were performed with collagen-coated chemotaxis μ-slides (Ibidi, Martinsried, Germany) according to the manufacturer's protocol. HepG2iso cells (1×10^6 cells/ml) were seeded onto the slides and 24 h later gradients (10–200 ng/ml) were generated with recombinant CXCL12.

Fibrin bead assay. The assay was performed as described previously,[49] except that CXCL12 and/or HA were used as indicated. Pictures were taken with an Olympus IX81 confocal microscope ($\times 2$ objective). A detailed protocol is available on request. The number of sprouts was counted and their length was measured using ImageJ (Bethesda, MA, USA).

Mouse aortic ring cultures. Aortic ring assays were performed as described previously[50] using aortas from 8- to 10-week-old C57BL/6 mice, except that CXCL12, sHA, HYL, KM81 or IgG were added as indicated. Aortic rings were photographed on day 10 using a Canon Power Shot S620 digital camera connected to an Axiovert 40c Zeiss microscope and evaluated using ImageJ.

Matrigel plug assay. Growth factor-reduced matrigel (BD Biosciences, Heidelberg, Germany) was mixed with CXCL12 (200 ng/ml), Healon (400 μg/ml), sHA (1 μg/ml), KM81 antibody or IgG (100 μg/ml) as indicated. Aliquots of these mixtures (300 μl) were injected subcutaneously into both flanks of C57Bl/6 mice. After 21 days, matrigel plugs were removed, fixed in zinc buffer and embedded in paraffin. Paraffin sections were stained with a rat anti-mouse CD31 antibody (0.5 μg/ml; BD Pharmingen, Heidelberg, Germany), anti-rat Alexa Fluor 546 (Invitrogen) and DAPI (Dako).

Conflict of Interest

The authors declare no conflict of interest.

Acknowledgements. This work was supported by grants of the Deutsche Forschungsgemeinschaft (SPP1190 'Tumor vessel interface', OR/JPS/BH).

Author Contributions

KF: performed the research, analyzed and interpreted the data; AH: performed part of the research, analyzed and interpreted the data; AS: performed part of the research, analyzed and interpreted the data; BH: critically read the manuscript; JPS: critically read the manuscript and contributed to the writing; VO-R: designed the research, analyzed and interpreted the data and wrote the paper.

1. Sleeman JP, Christofori G, Fodde R, Collard JG, Berx G, Decraene C *et al.* Concepts of metastasis in flux: the stromal progression model. *Semin Cancer Biol* 2012; **22**: 174–186.
2. Sleeman JP. The metastatic niche and stromal progression. *Cancer Metastasis Rev* 2012; **31**: 429–440.
3. Toole BP. Hyaluronan and its binding proteins, the hyaladherins. *Curr Opin Cell Biol* 1990; **2**: 839–844.
4. Slevin M, Krupinski J, Gaffney J, Matou S, West D, Delisser H *et al.* Hyaluronan-mediated angiogenesis in vascular disease: uncovering RHAMM and CD44 receptor signaling pathways. *Matrix Biol* 2007; **26**: 58–68.
5. Anttila MA, Tammi RH, Tammi MI, Syrjanen KJ, Saarikoski SV, Kosma VM. High levels of stromal hyaluronan predict poor disease outcome in epithelial ovarian cancer. *Cancer Res* 2000; **60**: 150–155.
6. Auvinen P, Tammi R, Parkkinen J, Tammi M, Agren U, Johansson R *et al.* Hyaluronan in peritumoral stroma and malignant cells associates with breast cancer spreading and predicts survival. *Am J Pathol* 2000; **156**: 529–536.
7. Lokeshwar VB, Rubinowicz D, Schroeder GL, Forgacs E, Minna JD, Block NL *et al.* Stromal and epithelial expression of tumor markers hyaluronic acid and HYAL1 hyaluronidase in prostate cancer. *J Biol Chem* 2001; **276**: 11922–11932.
8. Ropponen K, Tammi M, Parkkinen J, Eskelinen M, Tammi R, Lipponen P *et al.* Tumor cell-associated hyaluronan as an unfavorable prognostic factor in colorectal cancer. *Cancer Res* 1998; **58**: 342–347.
9. Setala LP, Tammi MI, Tammi RH, Eskelinen MJ, Lipponen PK, Agren UM *et al.* Hyaluronan expression in gastric cancer cells is associated with local and nodal spread and reduced survival rate. *Br J Cancer* 1999; **79**: 1133–1138.
10. Toole BP. Hyaluronan: from extracellular glue to pericellular cue. *Nat Rev Cancer* 2004; **4**: 528–539.
11. Ekici S, Cerwinka WH, Duncan R, Gomez P, Civantos F, Soloway MS *et al.* Comparison of the prognostic potential of hyaluronic acid, hyaluronidase (HYAL-1), CD44v6 and microvessel density for prostate cancer. *Int J Cancer* 2004; **112**: 121–129.
12. Simpson MA, Lokeshwar VB. Hyaluronan and hyaluronidase in genitourinary tumors. *Front Biosci* 2008; **13**: 5664–5680.
13. Stern R. Hyaluronan metabolism: a major paradox in cancer biology. *Pathol Biol (Paris)* 2005; **53**: 372–382.
14. Udabage L, Brownlee GR, Nilsson SK, Brown TJ. The over-expression of HAS2, Hyal-2 and CD44 is implicated in the invasiveness of breast cancer. *Exp Cell Res* 2005; **310**: 205–217.
15. Bharadwaj AG, Kovar JL, Loughman E, Elowsky C, Oakley GG, Simpson MA. Spontaneous metastasis of prostate cancer is promoted by excess hyaluronan synthesis and processing. *Am J Pathol* 2009; **174**: 1027–1036.
16. Enegd B, King JA, Stylli S, Paradiso L, Kaye AH, Novak U. Overexpression of hyaluronan synthase-2 reduces the tumorigenic potential of glioma cells lacking hyaluronidase activity. *Neurosurgery* 2002; **50**: 1311–1318.
17. Itano N, Sawai T, Atsumi F, Miyaishi O, Taniguchi S, Kannagi R *et al.* Selective expression and functional characteristics of three mammalian hyaluronan synthases in oncogenic malignant transformation. *J Biol Chem* 2004; **279**: 18679–18687.
18. Zhang L, Underhill CB, Chen L. Hyaluronan on the surface of tumor cells is correlated with metastatic behavior. *Cancer Res* 1995; **55**: 428–433.
19. Simpson MA. Concurrent expression of hyaluronan biosynthetic and processing enzymes promotes growth and vascularization of prostate tumors in mice. *Am J Pathol* 2006; **169**: 247–257.
20. Ghatak S, Misra S, Toole BP. Hyaluronan oligosaccharides inhibit anchorage-independent growth of tumor cells by suppressing the phosphoinositide 3-kinase/Akt cell survival pathway. *J Biol Chem* 2002; **277**: 38013–38020.
21. Zeng C, Toole BP, Kinney SD, Kuo JW, Stamenkovic I. Inhibition of tumor growth in vivo by hyaluronan oligomers. *Int J Cancer* 1998; **77**: 396–401.
22. Orian-Rousseau V, Ponta H. Adhesion proteins meet receptors: a common theme? *Adv Cancer Res* 2008; **101**: 63–92.
23. Savani RC, Cao G, Pooler PM, Zaman A, Zhou Z, DeLisser HM. Differential involvement of the hyaluronan (HA) receptors CD44 and receptor for HA-mediated motility in endothelial cell function and angiogenesis. *J Biol Chem* 2001; **276**: 36770–36778.
24. Cao G, Savani RC, Fehrenbach M, Lyons C, Zhang L, Coukos G *et al.* Involvement of endothelial CD44 during *in vivo* angiogenesis. *Am J Pathol* 2006; **169**: 325–336.
25. Tremmel M, Matzke A, Albrecht I, Laib AM, Olaku V, Ballmer-Hofer K *et al.* A CD44v6 peptide reveals a role of CD44 in VEGFR-2 signaling and angiogenesis. *Blood* 2009; **114**: 5236–5244.
26. Salcedo R, Oppenheim JJ. Role of chemokines in angiogenesis: CXCL12/SDF-1 and CXCR4 interaction, a key regulator of endothelial cell responses. *Microcirculation* 2003; **10**: 359–370.
27. Petit I, Jin D, Rafii S. The SDF-1-CXCR4 signaling pathway: a molecular hub modulating neo-angiogenesis. *Trends Immunol* 2007; **28**: 299–307.
28. Avigdor A, Goichberg P, Shivtiel S, Dar A, Peled A, Samira S *et al.* CD44 and hyaluronic acid cooperate with SDF-1 in the trafficking of human CD34 + stem/progenitor cells to bone marrow. *Blood* 2004; **103**: 2981–2989.

29. Burger JA, Kipps TJ. CXCR4: a key receptor in the crosstalk between tumor cells and their microenvironment. *Blood* 2006; **107**: 1761–1767.
30. Jin L, Hope KJ, Zhai Q, Smadja-Joffe F, Dick JE. Targeting of CD44 eradicates human acute myeloid leukemic stem cells. *Nat Med* 2006; **12**: 1167–1174.
31. Gassmann P, Haier J, Schluter K, Domikowsky B, Wendel C, Wiesner U *et al.* CXCR4 regulates the early extravasation of metastatic tumor cells *in vivo*. *Neoplasia* 2009; **11**: 651–661.
32. Orian-Rousseau V. CD44, a therapeutic target for metastasising tumours. *Eur J Cancer* 2010; **46**: 1271–1277.
33. Olaku V, Matzke A, Mitchell C, Hasenauer S, Sakkaravarthi A, Pace G *et al.* c-Met recruits ICAM-1 as a coreceptor to compensate for the loss of CD44 in Cd44 null mice. *Mol Biol Cell* 2011; **22**: 2777–2786.
34. Teicher BA, Fricker SP. CXCL12 (SDF-1)/CXCR4 pathway in cancer. *Clin Cancer Res* 2010; **16**: 2927–2931.
35. Post GR, Brown JH. G protein-coupled receptors and signaling pathways regulating growth responses. *FASEB J* 1996; **10**: 741–749.
36. Ho TK, Shiwen X, Abraham D, Tsui J, Baker D. Stromal-cell-derived factor-1 (SDF-1)/CXCL12 as potential target of therapeutic angiogenesis in critical leg ischaemia. *Cardiol Res Pract* 2012; **2012**: 143209.
37. Toole BP. Hyaluronan-CD44 interactions in cancer: paradoxes and possibilities. *Clin Cancer Res* 2009; **15**: 7462–7468.
38. Underhill CB, Chi-Rosso G, Toole BP. Effects of detergent solubilization on the hyaluronate-binding protein from membranes of simian virus 40-transformed 3T3 cells. *J Biol Chem* 1983; **258**: 8086–8091.
39. Zheng Z, Katoh S, He Q, Oritani K, Miyake K, Lesley J *et al.* Monoclonal antibodies to CD44 and their influence on hyaluronan recognition. *J Cell Biol* 1995; **130**: 485–495.
40. Jung T, Gross W, Zoller M. CD44v6 coordinates tumor matrix-triggered motility and apoptosis resistance. *J Biol Chem* 2011; **286**: 15862–15874.
41. Guleng B, Tateishi K, Ohta M, Kanai F, Jazag A, Ijichi H *et al.* Blockade of the stromal cell-derived factor-1/CXCR4 axis attenuates *in vivo* tumor growth by inhibiting angiogenesis in a vascular endothelial growth factor-independent manner. *Cancer Res* 2005; **65**: 5864–5871.
42. Hristov M, Zernecke A, Liehn EA, Weber C. Regulation of endothelial progenitor cell homing after arterial injury. *Thromb Haemost* 2007; **98**: 274–277.
43. Purcell BP, Elser JA, Mu A, Margulies KB, Burdick JA. Synergistic effects of SDF-1alpha chemokine and hyaluronic acid release from degradable hydrogels on directing bone marrow derived cell homing to the myocardium. *Biomaterials* 2012; **33**: 7849–7857.
44. Yang C, Cao M, Liu H, He Y, Xu J, Du Y *et al.* The high and low molecular weight forms of hyaluronan have distinct effects on CD44 clustering. *J Biol Chem* 2012; **287**: 43094–43107.
45. Kuschert GS, Coulin F, Power CA, Proudfoot AE, Hubbard RE, Hoogewerf AJ *et al.* Glycosaminoglycans interact selectively with chemokines and modulate receptor binding and cellular responses. *Biochemistry* 1999; **38**: 12959–12968.
46. Toole BP. Hyaluronan promotes the malignant phenotype. *Glycobiology* 2002; **12**: 37R–42R.
47. Csoka AB, Frost GI, Heng HH, Scherer SW, Mohapatra G, Stern R. The hyaluronidase gene HYAL1 maps to chromosome 3p21.2-p21.3 in human and 9F1-F2 in mouse, a conserved candidate tumor suppressor locus. *Genomics* 1998; **48**: 63–70.
48. Termeer C, Benedix F, Sleeman J, Fieber C, Voith U, Ahrens T *et al.* Oligosaccharides of Hyaluronan activate dendritic cells via toll-like receptor 4. *J Exp Med* 2002; **195**: 99–111.
49. Nakatsu MN, Sainson RC, Aoto JN, Taylor KL, Aitkenhead M, Perez-del-Pulgar S *et al.* Angiogenic sprouting and capillary lumen formation modeled by human umbilical vein endothelial cells (HUVEC) in fibrin gels: the role of fibroblasts and Angiopoietin-1. *Microvasc Res* 2003; **66**: 102–112.
50. Masson VV, Devy L, Grignet-Debrus C, Bernt S, Bajou K, Blacher S *et al.* Mouse aortic ring assay: a new approach of the molecular genetics of angiogenesis. *Biol Proced Online* 2002; **4**: 24–31.